Analysis of gamma-ray spectra with spectral unmixing, Part II: Recalibration for the quantitative analysis of HPGe measurements

Jiaxin Xu, Jérôme Bobin, Anne de Vismes Ott, Christophe Bobin, Paul Malfrait

Journal Pre-proof

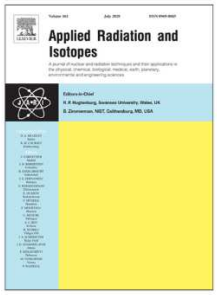

Analysis of gamma-ray spectra with spectral unmixing, Part II: Recalibration for the quantitative analysis of HPGe measurements

Jiaxin Xu, Jérôme Bobin, Anne de Vismes Ott, Christophe Bobin, Paul Malfrait

PII: S0969-8043(21)00472-3
DOI: https://doi.org/10.1016/j.apradiso.2021.110082
Reference: ARI 110082

To appear in: *Applied Radiation and Isotopes*

Received date : 3 March 2021
Revised date : 20 December 2021
Accepted date : 22 December 2021

Please cite this article as: J. Xu, J. Bobin, A. de Vismes Ott et al., Analysis of gamma-ray spectra with spectral unmixing, Part II: Recalibration for the quantitative analysis of HPGe measurements. *Applied Radiation and Isotopes* (2022), doi: https://doi.org/10.1016/j.apradiso.2021.110082.

Analysis of gamma-ray spectra with spectral unmixing - Part II: recalibration for the quantitative analysis of HPGe measurements

Jiaxin Xu[a], Jérôme Bobin[b], Anne de Vismes Ott[a,*], Christophe Bobin[c], Paul Malfrait[a]

[a] *Institut de Radioprotection et de Sûreté Nucléaire (IRSN), PSE-ENV, SAME, LMRE, F-91400 Orsay, France*
[b] *IRFU, CEA, Université Paris-Saclay, F-91191 Gif-sur-Yvette, France*
[c] *Université Paris-Saclay, CEA, List, Laboratoire National Henri Becquerel (LNE-LNHB), F-91120 Palaiseau, France*

Abstract

In the context of radioactivity measurements, the quantitative analysis of a gamma-ray spectrum depends on the analysis algorithm. To that end, we recently introduced a Poisson statistics-based spectral unmixing approach. However, it also relies on a proper instrument recalibration as well as on an uncertainty estimation, for which no solution has been proposed so far. The goal of this article is twofold: i) we first present a novel method to correct for the instrument calibration of an HPGe detection system, which is tailored to spectral unmixing algorithms, and ii) we apply this new approach to the quantitative analysis of real data as well as on the evaluation of the uncertainty. Along with the characteristic limits determination investigated, this paper introduces the first full metrological analysis sequence of aerosol filter measurements based on spectral unmixing, which allows to quantify both the radionuclides' activities and their associated uncertainties.

Keywords: gamma-ray spectrometry, calibration, full spectrum analysis, Poisson statistics-based spectral unmixing, metrological analysis

*Corresponding author
Email address: anne.de-vismes@irsn.fr (Anne de Vismes Ott)

1. Introduction

Gamma-ray spectrometry is a widely used technique for the determination of radioactivity in some sample (*e.g.*, aerosol, soil, water, etc.). The main challenge of gamma-ray spectrum analysis is the need for the rapid detection of radionuclides, which requires more efficient activity estimation methods. In line with this objective, the Poisson statistics-based spectral unmixing (Xu et al., 2020) has been developed as a new gamma-ray spectrum analysis tool, which allows providing a precise and sensitive activity estimation of radionuclides.

In order to achieve a truly metrological analysis with spectral unmixing, we need two key ingredients: the first one is the determination of characteristic limits with precise statistical analysis tools, which has been thoroughly investigated in Xu et al. (2021). The second ingredient, which is key to apply the spectral unmixing to real data analysis, is instrument recalibration.

In contrast to standard peak-based methods, spectral unmixing considers the full energy range of a measured gamma-ray spectrum. In the next, the spectrum is assumed to be composed of M channels: $\boldsymbol{x} = [x_1, ...x_M]$.The background spectrum is denoted by $\boldsymbol{b}$ and the spectral signatures of radionuclides by $\boldsymbol{\Phi} = [\boldsymbol{\phi}_1, ...\boldsymbol{\phi}_N]$. The mixing weights are defined by $\boldsymbol{a} = [a_1, ...a_N]$. Each column of $\boldsymbol{\Phi}$ represents the spectral signature of a radionuclide and N is the number of radionuclides. The underlying detection process leads to the following model:

$$x_i \sim \mathcal{P}oisson\left([\boldsymbol{\Phi a}]_i + b_i\right) \tag{1}$$

As described in Xu et al. (2021), the activity estimation problem is equivalent to the estimation of the mixing weights vector from an estimator that maximizes the likelihood of the above Poisson distribution, which leads to minimizing the following neg-log-likelihood:

$$\hat{\boldsymbol{a}} = \underset{\boldsymbol{a}}{\operatorname{argmin}}\, \boldsymbol{\Phi a} + \boldsymbol{b} - \boldsymbol{x} \odot \log\left(\boldsymbol{\Phi a} + \boldsymbol{b}\right) \tag{2}$$

where $\odot$ is the Hadamard product (*i.e.* the element-wise product).

Such Poisson-statistics based spectral unmixing has been shown to provide a more accurate estimation of $\boldsymbol{a}$ than the peak-based spectrum analysis (Xu

et al., 2020). Since spectral unmixing analysis radically differs from standard peak-based analysis, designing a fully metrological analysis is not straightforward. As emphasized (Xu et al., 2020), spectral unmixing methods strongly rely on the availability of spectral signatures, regardless if they originate from simulations or of measurement single-gamma-ray emitters. However, the analysis of complex spectra with radionuclides that are hard to produce in mono-energetic sources makes the use of simulation-based spectral spectra necessary. In this case, using full spectrum analysis methods requires correcting the calibration of the spectral signatures in the full energy range. To achieve an accurate quantitative analysis, we investigate more specifically how to correct the spectral signatures in resolution, efficiency and energy, making possible the application of the spectral unmixing method to analyze spectra of environmental aerosol filter measurements performed with HPGe gamma-ray detectors investigated in Xu et al. (2020). The proposed procedure will be validated with spectra measured with a given detection system (*i.e.*, detector and source geometry), which can be virtually applied to other detection systems that provide spectra with sufficient energy resolution (*e.g.* NaI(Tl) or LaBr3 scintillator detectors).

The contribution of this paper is organized as follows: in Section 2, we introduce an instrument recalibration procedure that is adapted to the spectral unmixing algorithm. Next, in Section 3, we detail each step of the instrument recalibration method. In Section 4, after validating the proposed method with the analysis of a standard multi-gamma source (*i.e.*, with known radionuclides' activities and uncertainties), we apply the proposed analysis sequence to analyze past measurements of environmental aerosol filters samples and compare the results to those obtained with the standard method using the Genie2000 (Mirion-Canberra, 2016) spectrum analysis software. Finally, Section 5 provides conclusions and perspectives of this work.

2. Towards instrument recalibration for spectral unmixing

Given a measured gamma-ray spectrum, with peak-based analysis, the activity estimation of radionuclides is based on the detected counts in their corresponding full energy peaks. Such Regions of Interest (ROI) analysis is described in Gilmore (2008). The full spectrum analysis estimates the activities through their detected counts in the full energy range. Both of these two procedures require the instrument to be calibrated, so as to precisely relate the detected counts to radionuclides' activities. Fig. 1 illustrates an example of a gamma-ray spectrum of aerosol measurement performed with HPGe detector. The major peaks are related to the main radionuclides present in decreasing activity levels : ^{7}Be at 477 keV, ^{210}Pb at 46.5 keV, ^{40}K at 1460 keV, ^{22}Na at 1274 keV, ^{137}Cs at 662 keV, in addition to those present in the background (^{214}Pb, ^{214}Bi,...). Whether it is for the identification of the radionuclides or the quantification of their activities, three recalibration steps need to be addressed:

- **Energy:** In practice, energy calibration is done at the installation with a standard source. An energy recalibration is performed for each sample measurement using the peaks of the present natural radionuclides to correct the shift in peak positions due to the electronics drift.
- **Efficiency and resolution:** For the quantification purpose, it is customary to use multi-gamma sources of known activities to describe the full energy peak detection efficiency and the shape of energy peaks (*i.e.*, resolution specified by the full width at half maximum of the peaks) as a function of energy.

As described in Section 1, in the gamma-ray spectrum mixing model, the detected number of counts in each channel due to a radionuclide correspond to columns of the matrix $\mathbf{\Phi}$ multiplied by their mixing weights: $[\phi_1 a_1, ...\phi_N a_N]$, where N is the number of radionuclides. Assuming that the spectral signatures $[\phi_1, ...\phi_N]$ are known, the radionuclides' activities are therefore proportional to the mixing weights $[a_1, ...a_N]$. In this context, the calibration raises two major

challenges:

1. In practice, the radionuclides contained in environmental samples are rarely present in standard sources. The spectral signatures therefore need to be simulated. One primary problem of using simulated spectral signatures is to ensure that the simulations reproduce the actual responses of the detection system in terms of the energy bins (*i.e.* the intervals of energy corresponding to single channels of the measured spectra), the efficiency and the resolution.
2. Another key problem is how to relate the mixing weights to radionuclides' activities. Throughout this paper, we make use of the MCNP particle transport code (Briesmeister, 2000), which simulates the interaction between the gamma-rays and the materials of the detection system and finally normalizes the spectrum by the number of source-particle histories run in the simulation process.

   The simulation of radionuclides' spectral signatures is performed with the MCNP-CP (A Correlated Particle Radiation Source Extension of a General Purpose Monte Carlo N-Particle Transport Code (Berlizov, 2006)), which uses the full decay scheme including the gamma emission probability and simulates the physics of nuclear decay and the subsequent emissions of each radionuclide using the data from the Evaluated Nuclear Structure Data File (ENSDF) of the National Nuclear Data Center (Brookhaven National Laboratory). While MCNP simulates photons of a given energy, MCNP-CP simulates the emissions of a given radionuclide. In this case each simulated spectral signature corresponds to the spectrum obtained for 1 disintegration of the radionuclide (i.e. 1 becquerel measured for 1 second). Therefore, the estimated mixing weight of each radionuclide corresponds to its number of disintegrations. This leads to quantify the radionuclides' activities with:

$$\hat{\boldsymbol{g}} = \frac{\hat{\boldsymbol{a}}}{t} \tag{3}$$

   where $\hat{\boldsymbol{a}}$ and t stand for the vector of estimated mixing weights described

in Section 1 and the counting time of the measurement. The vector $\hat{\boldsymbol{g}}$ contains the radionuclides' activities in becquerel (Bq) (*i.e.*, number of disintegrations per second).

3. Instrument calibration correction in spectral unmixing, a two-step approach

As we discussed in Section 2, the simulation of spectral signatures $\boldsymbol{\Phi}$ needs to be adjusted so as to account for the accurate experimental features of the detection system (*i.e.* detector and source geometry). In the same spirit of standard peak-based analysis instrument calibration, we consider the energy, efficiency and resolution calibration. Indeed the spectral signatures are obtained by simulating the detector response using the MCNP "F8" pulse height tally. This is the distribution of the pulse heights and thus the total energy deposited in a cell (*i.e.*, the crystal detector) in equal-width energy bins.

In this context, the calibration correction for the detection efficiency and resolution can be done by adjusting the model of the experimental arrangement of spectral signatures with a standard source. Furthermore, an energy calibration refinement step of the spectral signatures is needed during the analysis, since the MCNP code computes simulated energy response in small identical width energy bins, which means that the energy and the channel number are linearly dependent. In contrast, the relationship between the energy and the channel number $E = f(\text{channel})$ is non-linear for measured spectra. Fig. 2 shows an example of energy bin width of a measured spectrum and a simulated spectrum. To ensure that the simulated spectral signatures correspond to energy responses at the exact same energy bins of the measured spectrum, we propose a new energy calibration refinement algorithm, which applies during the spectral unmixing analysis.

3.1. Data description

In this work, we particularly focus on processing the data produced by one of the 23 HPGe detection systems of the IRSN/LMRE laboratory. The ex-

perimental set-up consists of a gamma-ray spectrometer with a BEGe 5030 (Broad Energy Germanium, MIRION-Canberra) detector (crystal dimensions: $\emptyset$ = 80mm, h = 30mm) calibrated to measure radionuclides emitting photons with energies ranging from 20 keV to 1700 keV, and a DSA-1000 (Canberra) multi-channel analyzer based upon digital signal processing using 16384 channels, i.e. around 0.1 keV per channel. Fig. 3 shows the MCNP simulation model of the actual detector. The Genie 2000 (Mirion-Canberra, 2016) software (version 3.4.1) is used for both spectra acquisition and routine analysis. The system has a relative efficiency of 61% and a resolution of 0.54 keV, 1.2 keV and 1.7 keV at 46 keV, 622 keV and 1460 keV, respectively. The detector is surrounded by a 5cm thick lead shield, and equipped by an anti-cosmic system consisting in 5 scintillating plastic plates (5 cm thick). The volume of the cavity of the inner lead shield is optimized to be as small as possible to avoid radon concentration : it is 20 x 15 x 30 cm^3. Furthermore the whole system is installed in a 20 m^2 shallow shielded room made of 10 cm lead bricks and internally lined by 5 mm oxygen-free copper to stop the X-rays emitting by the lead desexcitation, in the second basement of the laboratory, under a 10 m w.e. (meter water equivalent) borated concrete slab. These facilities and equipments reduce both telluric and cosmic components of the radiological background. Finally the inner measurement chamber is flushed by the gaseous nitrogen escaping from the liquid nitrogen dewar to reduce and stabilize the radon induced background. The sampled aerosol filters are dried for 24 hours before being pressed into pellets, weighted and then packaged in 10 mL cylindrical counting geometries (dimensions: $\emptyset$ = 52mm, h = 4.7mm). The container is packaged in a plastic bag and put on the detector window protected by a Petri box endcap to avoid contamination. This measurement directly on the detector endcap maximizes the detection efficiency. All the aerosol filters are measured after at least 4 days and generally one week, except in case of particular event, in order to wait the decay of the radon progeny and to decrease significantly the decision threshold of ^{137}Cs and thus increase the detection rate of this radionuclide of interest.

Calibration corrections are carried out with a multi-gamma standard source

of known activities, which contains ^{51}Cr, ^{57}Co, ^{60}Co, ^{85}Sr, ^{88}Y, ^{109}Cd, ^{113}Sn, ^{137}Cs, ^{139}Ce, ^{210}Pb, ^{241}Am. This source is made of a mixture of liquid radioactive solutions and epoxy resin ; it is water equivalent in terms of photons attenuation and its density is 1.15 g.cm^{-3} The source dimensions are $h = 4.64$mm, $\emptyset = 52$mm and it is contained in the 10 mL container. The gamma-ray spectrum measured for this source is shown in Fig. 4.

It should be noted that the instrument recalibration that we investigate in this work can also be applied to other detection systems for the activity quantification.

3.2. Simulation adjustments for the detection efficiency and resolution

The simulation of the radionuclides' spectral signatures are performed with the MCNP-CP code described in Section 2. The total number of source particle histories run in each simulation is 10^9 within an energy range of 20 keV to 2740 keV. The equal-width energy bins are set to 0.1 keV.

Efficiency recalibration. For a given radionuclide, the simulated spectrum has one or several peaks and their associated continua. The calibration correction of the total detection efficiency related to the number of counts in the full spectrum (*i.e.*, peaks and continua) cannot be generated as a function of energy, since the spectral features are different for radionuclides at the same energy. Therefore, we consider the full energy peak efficiency recalibration (noted as FEPE) in the full energy range with the given multi-gamma standard source.

More precisely, we aim to simulate energy responses that provide a good agreement of the FEPE (hereafter noted as efficiency) for each peak of the source measurement (shown in blue in Fig. 4). Since the MCNP-CP code takes into account the true coincidence summing effect in the simulation of the detector's energy response, the efficiency recalibration can be performed with two steps considering the full energy peak efficiencies uncorrected from the true coincidence effect, for both experimental and simulated efficiencies :

- **Experimental efficiencies:** we firstly determine the experimental efficiencies for some peaks of each radionuclide. This is done by analyzing the standard source with a peak-based analysis methods. The efficiency of the energy peak e of the considered radionuclide is then determined by:

$$\epsilon^{exp}(e) = \frac{N_p(e)}{A(e) \times I(e) \times t} \tag{4}$$

where $N_p(e)$ is the number of observed counts in this full energy peak e, $A(e)$ is the activity of the radionuclide that emits photons at this energy, which is known for the standard source, I is the intensity of this energy peak (*i.e.* the number of emitted photons of the corresponding gamma-ray for 100 disintegrations of the radionuclide) and t is the counting time of the measurement.

- **Calculated efficiencies:** next, simulations are performed individually for each radionuclide that composes the source. Knowing that the simulated response is normalized by the number of particles run in the simulation, the detection efficiency of a full energy peak e of the simulated detection system is:

$$\epsilon^{simu}(e) = \frac{H(e)}{I(e)} \tag{5}$$

In this case MCNP-CP is used without the GEB (Gaussian Energy Broadening) card and the full energy peak is a Dirac distribution ; the calculated FEPE can thus be directly determined from the the peak height $H(e)$ and emission probability $I(e)$ according to e according to equation 5.

The simulation configurations are set to the dimension and material features of the detection system shown in Fig. 3. They are slightly tuned so as to provide better agreement of ϵ^{exp} and ϵ^{simu}. The crystal length has been changed from the nominal value given by the supplier, from 31 mm to 28 mm, while the distance between the germanium crystal front to inside endcap window, 5 mm, was not changed. This size reduction induces a decrease of the detection efficiency for the high energy range photons. The thickness of the germanium

entrance window, also called dead layer, has been increased, from 0.4 μm to 13 μm to slightly decrease the calculated detection efficiency for low energy range photons.

For comparison purposes, the full energy peak efficiency of the radionuclides in the reference source, noted ϵ^{exp} and the full energy efficiency calculated with MCNP-CP simulations, noted ϵ^{simu}, we display the ratio $\frac{\epsilon^{simu}}{\epsilon^{exp}}$ at each peak energy in Fig. 5.

As a result, the full energy peak efficiency ratio shows an agreement of less than 5 % error for all the peaks, which will be taken into account to quantify the uncertainty of the measurement.

Resolution calibration correction for spectral unmixing. The detection resolution is an important feature of gamma-ray measurements, for which the calibration is particularly important for the analysis of HPGe measurements since the number of counts is large in the few channels of the peaks. In the MCNP-CP input file, the resolution can be specified with the Gaussian Energy Broadening (GEB) special feature, which describes the shape of energy peaks as a function of energy:

$$FWHM = a + b\sqrt{(e + c.e^2)} \tag{6}$$

where e is the full energy peak energy and FWHM represents the Full Width at Half Maximum of the peak. The parameters in the empirical model Eq. (6) need to be determined in this step.

More precisely, we measure the FWHM of different full-energy peaks, which leads to the experimental data points: $[\boldsymbol{e}, \boldsymbol{r}]$. $\boldsymbol{e}$ and $\boldsymbol{r}$ are the peaks' energies and their corresponding $FWHM$ values, respectively. Then, we make use of these points to fit the empirical model in the form of Eq.(6) to find the parameters a,b and c in the model.

Fig. 6 compares the $FWHM$ values of the measured spectrum and those specified in the simulations. The comparison shows a good agreement of the peak width in the simulations. However, the model is less efficient to fit the

peak at 21.9 keV, which is of X-ray origin. It should be noted that X-rays at low energies have larger peak width and can not be well calibrated with the empirical function Eq. (6). Nevertheless, spectral unmixing is usually performed for energy higher than 40 keV for gamma-ray spectral analysis of aerosol measurements, where the simulation allows to produce good spectral responses in terms of detection resolution.

Complexity of the spectral signatures. The interaction of photons, emitted by the source or coming from the surrounding background, with the lead shielding induces the emission of X-rays of Pb; this should be considered in the library of spectral signatures used to unmix an HPGe gamma-ray spectrum.

Nevertheless, we are not interested in the quantification of these spectral components since they are present whatever radionuclides are present in the sample, their counting rates are only related to the total photon number emitted by the sample and their energies, but can not be used to determine the activity of any radionuclide. An additional spectral signature is therefore considered, which is simulated using the MC method for the mixture of X-rays of Pb at 72.8 keV (60 %), 75 keV (100 %), 84.4 keV (12 %), 84.9 keV (23 %) and 87.3 keV (8 %) with their respective emission intensity.

3.3. Energy calibration refinement

For a measured gamma-ray spectrum, the energy recalibration is practically performed by localizing peaks of known energies. It has recently been proposed in Wang et al. (2021) to recalibrate the energy scale of a measured spectrum by fitting a non-linear function. In the context of spectral unmixing, we rather focus on correcting the spectral signatures. This approach raises the following practical issues:

- As the simulated spectral signatures can not be calculated at exactly the same energies than the measured spectrum, they need to be interpolated to the measurement energy bins.

- Estimation bias can be caused by the shift of energy between a measured spectrum and recalibrated spectral signatures.

To overcome these problems, we propose to use high-resolution (interpolated) simulated spectral signatures, with finer channel widths. Then, we propose a calibration refinement step that allows correcting the energy shift due to the interpolation. The aim of using a high resolution domain is to precisely determine the energy shift.

In this problem, we define two sampling operators as follows:

$$\mathbf{\Phi} = H\mathbf{\Phi}_{hr},\ \mathbf{\Phi}_{hr} = L\mathbf{\Phi} \tag{7}$$

where $\mathbf{\Phi}$ and $\mathbf{\Phi}_{hr}$ represent spectral signatures respectively in actual energy domain and high resolution domain. Note that E and E_{hr} are energy bins of $\mathbf{\Phi}$ and $\mathbf{\Phi}_{hr}$. The operator H and L correspond to the sampling operators of $E_{hr} \to E$ and $E \to E_{hr}$ respectively.

More precisely, the energy calibration refinement for the analysis of the mentioned standard source is described as follows:

Step 1: Interpolation of simulated spectral signatures. In the MCNP simulation process, the energy bin width of simulated spectra is set to an interval of 0.1 keV (*i.e.*, simulation of energy responses at each 0.1 keV). This matrix of simulated spectral signatures is denoted as $\mathbf{\Phi}_{simu}$. As illustrated in Fig. 7, to analyze a measured spectrum $\boldsymbol{x}$ referring to Eq.(2), $\mathbf{\Phi}_{simu}$ need to be interpolated into the energy bins of $\boldsymbol{x}$. To this end, each simulated spectral signature in $\mathbf{\Phi}_{simu}$ is first interpolated into high resolution energy bins (see illustration in Fig. 7-a), with 10 energy bins in one channel (*i.e.*, energy responses at each 0.01 keV). The obtained high resolution spectral signatures is denoted as $\mathbf{\Phi}_{hr}$. Then $\mathbf{\Phi}_{hr}$ is interpolated into energy bins of $\boldsymbol{x}$ (see illustration in Fig. 7-b), noted $\mathbf{\Phi}_r$.

Step 2: First activity estimation. The spectral unmixing provides a first estimation of activities with $\mathbf{\Phi}_r$, which is denoted as $\hat{\boldsymbol{a}}_r$. The energy shift is

illustrated in Fig. 8 for a single peak. This energy shift varies in the full energy range. Therefore, we propose an energy refinement algorithm that accounts for the energy values of the available peaks.

Step 3: Quantification of energy shift. We aim to fit an energy refinement function from K peaks, noted $[e_0, ...e_K]$, for which the energies are known. To estimate the energy shift of each peak, we propose to seek the optimal shift value in a given range. More precisely, we define a maximum number of shift steps in the high resolution domain, which is fixed to $N_{max} = 15$ (*i.e.*, shift the spectrum to left or right with maximum 15 energy bins in the high resolution domain, which is according to 0.15 keV in our simulated response). As illustrated in Fig. 9, we shift the spectrum of the peak region for n steps, while $n < 0$ implies that we shift the spectrum to left and $n > 0$ inversely. Therefore, the energy shift of a peak can be obtained with the shift n that minimizes the estimation residual in the peak region. The details are given in the Algorithm 1: At each iteration, we first shift each spectral signatures $\mathbf{\Phi}_{hr}$ of n steps, the shifted library is denoted as $\mathbf{\Phi}_{hr}^{'}$. Then, we calculate the quadratic residual with $\mathbf{\Phi}_{hr}^{'}$.

Step 4: Energy correction function fitting. Once the energy shift of the peaks have been determined in step 3, we can perform the energy correction by fitting a polynomial function of degree 3 to the peaks energies. This empirical choice is motivated by the fact that, using 2 degree polynomial leads to under-fitting and using a higher-order polynomial does not provide better results and likely yields over-fitting.

It is advantageous to extract more information from the peaks that are better distinguished from other spectral contributions. Therefore, we propose to re-calibrate the spectral signatures' energy by solving the following weighted least squares problem that aims to fit a polynomial function with c_0, c_1, c_2, c_3.

$$\min \sum_{i=1}^{K} w_i \left(e_i + \Delta_e^i - (c_0 + c_1 e_i + c_2 e_i^2 + c_3 e_i^3)\right)^2 \tag{8}$$

where e_i is the photon energy of the i^{th} peak, $e_i + \Delta_e^i$ is the target energy of the i^{th} peak, and K is the number of peaks used in this recalibration step.

Algorithm 1 Energy shift determination for the i^{th} peak

for $-N_{max} < n < N_{max}$ **do**

- shift n step for $\mathbf{\Phi}_{hr}$, we obtain $\mathbf{\Phi}_{hr}^{'}$
- calculate the quadratic residual in the i^{th} peak:

$$r = \frac{\sum_{\text{channels in the } i^{th}\text{peak}} (\boldsymbol{x} - \boldsymbol{b} - H\mathbf{\Phi}_{hr}^{'}\hat{\boldsymbol{a}}_r)^2}{\text{number of channels in the } i^{th}\text{peak}}$$

  where $\boldsymbol{x}$ and $\boldsymbol{b}$ are the measured spectrum and the background spectrum. $\hat{\boldsymbol{a}}_r$ is the activity estimated in Step 2. H is the sampling operator described in Eq. (7).

end for

- Select the shift step n that minimizes the residual r
- calculate energy shift $\Delta_e^i = n\delta_e$, ($\delta_e = 0.01$ keV is the energy bin in high resolution domain in this experiment)

The weight of each peak is computed as follows:

$$w_i = \frac{1}{\sum_{\text{channels in the } i^{th}\text{peak}} m_i} \tag{9}$$

where $\boldsymbol{m}$ is the equivalent background with respect to other spectral contributions (radionuclides and background denoted as $\boldsymbol{b}$) except for the j^{th} radionuclide that emits photons at the i^{th} peak, which is defined as follows:

$$\boldsymbol{m} = \sum^{l \neq j} \boldsymbol{\phi}_l a_l + \boldsymbol{b} \tag{10}$$

To overcome this problem, we can write the coefficients with a vector $\boldsymbol{c} = [c_0, c_1, c_2, c_3]$, by considering the following matrix form:

- Vector $\boldsymbol{e} = [e_1, ...e_K]$ is the photon energies of the K peaks

- Matrix of variables in the polynomial function noted as:

$$\boldsymbol{V} = \begin{pmatrix} 1 & e_1 & e_1^2 & e_1^3 \\ . & . & . & . \\ . & . & . & . \\ 1 & e_K & e_K^2 & e_K^3 \end{pmatrix}$$

- Vector energy shift of peaks: $\Delta_e = [\Delta_e^1, ...\Delta_e^K]$ quantified in step 3.

- Weights matrix $\Sigma = \text{diag}\,(w_1, ...w_K)$

The coefficients can be calculated by solving the following problem:

$$\underset{\boldsymbol{c}}{\text{argmin}}(\boldsymbol{e} + \Delta_e - \boldsymbol{V}\boldsymbol{c})^T \Sigma^{-1} (\boldsymbol{e} + \Delta_e - \boldsymbol{V}\boldsymbol{c}) \tag{11}$$

which leads to:

$$\boldsymbol{c} = \left(\boldsymbol{V}^T \Sigma^{-1} \boldsymbol{V}\right)^{-1} \boldsymbol{V}^T \Sigma^{-1} \left(\boldsymbol{e} + \Delta_e\right) \tag{12}$$

The parameters determined for the multi-gamma source measurement are:

$$\boldsymbol{c} = [-0.0598, 0.9999, 9.38 \times 10^{-8}, -5.62 \times 10^{-11}]$$

Finally, the corrected spectral signatures $\boldsymbol{\Phi}$ can be obtained by interpolating the corrected energy bins (High resolution domain) at the energy bins of the measurement.

$$\boldsymbol{\Phi}_f = H\left(c_0 + c_1 E_{hr} + c_2 E_{hr}^2 + c_3 E_{hr}^3\right) \tag{13}$$

where H is the sampling operator described in Eq.(7), and $\boldsymbol{\Phi}_f$ is the final library containing the recalibrated signatures.

To evaluate the proposed energy refinement algorithm, the estimation residual is compared to results before and after energy correction. These residuals, which are normalized by the observed counts, are displayed for several peaks in Fig. 10. This result highlights that the energy shift correction improves the spectral unmixing, which has significant benefits by reducing the estimation

residual in peak regions of the spectrum. For the analysis of HPGe gamma-ray spectrum, where the counts in peaks regions are dominant, we can especially benefit from a significant improvement from this energy refinement step.

4. Experiments on aerosol measurements

In this section, we aim to first validate an analysis sequence including the proposed recalibration steps and characteristic limits assessment introduced in Xu et al. (2021). This is done by analyzing the spectrum of the standard source, in which the radionuclides' activities and associated uncertainties are known, are measured with the calibrated detection system. Next, we apply this analysis sequence to real data and compare the results with those obtained with standard peak-based analysis.

4.1. Uncertainty budget

Before proceeding with the spectral analysis, the main practical problem comes from the uncertainties of the measurements, which contain both statistical uncertainties related to the estimation procedure and systematic uncertainties related to the material and the instrument calibration. In practice, the uncertainties of the results are determined from the probability that the estimated activity is contained in an interval based on a given p-value γ, where $\gamma = 0.05$ is usually taken into account. More precisely, the standard deviation of the activity estimation noted as σ, the uncertainty is according to 2σ for the Normal distribution assumption (*i.e.* k=2). For this purpose, we make use of the relative uncertainties defined with:

$$u = \frac{2\sigma}{\hat{g}} \tag{14}$$

where $\hat{g}$ stands for the estimated activity. The relationship between $\hat{g}$ and the mixing weight is described in Eq.(3).

We establish an uncertainty budget by using the spectral unmixing, which contains the following uncertainty terms:

- In Xu et al. (2021), we propose to assess the statistical uncertainty from Fisher information matrix of the estimated mixing weights:

$$\boldsymbol{I}(\hat{\boldsymbol{a}}) = \boldsymbol{\Phi}_f^T \mathrm{diag}\big(\boldsymbol{x} \oslash (\boldsymbol{\Phi}_f \hat{\boldsymbol{a}} + \boldsymbol{b})^2\big) \boldsymbol{\Phi}_f \tag{15}$$

  where $\oslash$ is the element-wise division. $(\boldsymbol{\Phi}_f \hat{\boldsymbol{a}} + \boldsymbol{b})^2$ calculates the element-wise product between the vector and itself. The standard deviation of the maximum likelihood estimation distribution is approximated by $.sqrt(\boldsymbol{I}(\hat{\boldsymbol{a}})^{-1}_{ii})$, which denotes the i-th element on the diagonal of the inverse of the matrix $\boldsymbol{I}(\hat{\boldsymbol{a}})$

  This uncertainty term is calculated with:

$$u_{stat} = \frac{2\sigma_f}{\hat{a}}$$

  where σ_f and $\hat{a}$ stand for the standard deviation calculated from Fisher information matrix and the estimated mixing weights respectively.

- As investigated in Section 2, spectral signatures $\boldsymbol{\Phi}$ are calibrated with a relative uncertainty of 5%, noted as u_{calib}
- The uncertainty of the standard source that was used for the calibration: $u_{source} = 5\%$.
- The uncertainty needs to take into account the variability of the sample position, for which we take the same value as considered in Genie 2000 analysis in the laboratory $u_{sample\_pos} = 2\%$.
- The uncertainty associated with the variation of detection efficiency is monthly checked by quality controls $u_{detector} = 4\%$.

Assuming that these uncertainty terms are statistically independent, the total measurement uncertainty can be evaluated with their total sum:

$$u = \sqrt{u_{stat}^2 + u_{calib}^2 + u_{source}^2 + u_{sample-pos}^2 + u_{detector}^2} \tag{16}$$

4.2. Analysis validation with the standard source measurement

As a result, the activity estimation carried out with the Poisson based spectral unmixing are compared to the reference activities given by the source in Table 1. To further evaluate the results, we make use of the zeta-score (ζ_{score}) described in the ISO 13528 international standard, which evaluates the results obtained with spectral unmixing by measuring its distance from the reference values normalized as a standard normal distribution.

$$\zeta_{score} = \frac{\hat{g} - g_{ref}}{\sqrt{u^2 + \sigma_{ref}^2}} \tag{17}$$

where $\hat{g}$ and σ are the estimated activity and the standard uncertainty (according to $k = 1$ of Eq.(16)), g_{ref} and σ_{ref} represent the activity and uncertainty ($k = 1$) of the reference source.

As reported in Table 1, the ζ_{score} assessed for radionuclides of the standard source satisfies the following criteria:

- $|\zeta_{score}| \leq 2$ indicates "satisfactory"
- $2 \leq |\zeta_{score}| \leq 3$ indicates "questionable"
- $|\zeta_{score}| \geq 3$ indicates "unsatisfactory"

The evaluation of the spectral unmixing analysis with the standard source allows drawing the following conclusion: the activity and uncertainty estimation with the spectral unmixing method is able to provide quantitative analysis that are close to the reference values. It can be used to analyze the aerosol measurements performed with the same detection system.

4.3. Re-analysis of aerosol measurements

Analyzing environment radioactivity measurements is particularly challenging when the activity of low-level radionuclides needs to be estimated with high accuracy and high sensitivity. We make use of the proposed spectrum analysis sequence of the Poisson based spectral unmixing to re-analyze past measurements of environmental samples (aerosol filters) performed with the calibrated

detection system. The simulated spectrum of a typical aerosol measurement is shown in Fig. 11, which mainly consists of: ^{7}Be, ^{22}Na, ^{40}K, ^{137}Cs, ^{210}Pb.

The uncertainty terms to analyze spectra performed with the calibrated detection system has been assessed in Section 4.1. To analyze aerosol measurements, another uncertainty term associated with the variation of the pressed filter needs to be taken into account in the uncertainty budget. More precisely, due to the preparation process of aerosol samples, the thickness and the density of the pressed filter samples are different than those of the standard source, which leads to variations of the detection efficiency. More precisely, to analyze the aerosol measurements, we make use of the spectral signatures simulated with the median values of the thickness and the density of aerosol filters of past measurements to better reproduce the detector response. An uncertainty term of $u_{sample} = 4\%$ of the source geometry variation is added in the resulting activities of the spectral unmixing, *i.e.*, combining with other uncertainty terms in Eq.(16), which leads to:

$$u = \sqrt{u_{stat}^2 + u_{calib}^2 + u_{source}^2 + u_{sample-pos}^2 + u_{detector}^2 + u_{sample}^2} \tag{18}$$

In the next, we apply the spectral unmixing method we introduced in Xu et al. (2020), equipped with the proposed calibration correction procedure, to analyze 67 real aerosol spectra. These spectra have been measured during the past two years with the aforementioned calibrated HPGe detector. To that end, we make the following evaluations:

- The radionuclides' activities in Bq along with their associated measurement uncertainties.
- Decision threshold of each radionuclides derived from statistical test introduced in Xu et al. (2021) with $\alpha = 0.025$, which is also considered in the standard method used for routine analysis.

For comparison purposes, we focus on the activity estimation of ^{7}Be, ^{22}Na, ^{40}K, ^{137}Cs and ^{210}Pb resulting from the Poisson-based spectral unmixing and

Genie 2000. Fig. 12 shows the histogram of the ratio between the activities estimated with the spectral unmixing and Genie 2000:

$$r = \frac{\hat{g}_1}{\hat{g}_2} \tag{19}$$

where $\hat{g}_1$ stands for Poisson based spectral unmixing and $\hat{g}_2$ for Genie 2000. Additionally, Fig. 13 displays the activities estimated with Genie 2000 as a function of those estimated with Poisson based spectral unmixing, where the error bars represent the uncertainties of the results. The activity unit in these results is mBq $\pm$ uncertainty ($k = 2$).

These results allow to draw the following conclusion:

- In the case of ^{7}Be and ^{210}Pb, the estimated activities with the spectral unmixing are systematically lower than those obtained with Genie 2000. Similarly, it tends to be larger for ^{40}K. However, Figure 13 shows that for these 3 radionuclides both methods are in agreement within the $k = 2$ error bars.

- The case of ^{22}Na and ^{137}Cs is significantly different. Indeed, Fig. 12 shows that spectral unmixing yields larger activity estimations than Genie 2000 for these two radionuclides. Furthermore, this discrepancy is statistically significant as featured in Fig. 13.

  Different explanations can be considered; this discrepancy could originate from an imperfect recalibration. In the case of spectral unmixing this would result in a mismatch between the recalibrated spectral signatures and the actual response of the detector for a given radionuclide. If this were the dominant source of discrepancy between spectral unmixing and Genie 2000, it would also impact ^{40}K, ^{7}Be and ^{210}Pb. As well, this could also be observed in the analysis of the multi-gamma source, where both the recalibration procedure and the unmixing technique used are similar. In the case of the multi-gamma source, such a difference is not observed for ^{137}Cs.

  Another key difference between ^{22}Na and ^{137}Cs with respect to the other

three radionuclides is there activity is low with respect to the background. This means that they are observed at low signal-to-noise ratio. In the validation step we performed with a multi-gamma source, the activities are of tens or hundreds of becquerel, while activities of ^{137}Cs are usually in the order of tens of millibecquerel, even only few millibecquerels. One central difference between Genie 2000 and spectral unmixing is that the former precisely account for the Poisson nature of the noise. In (Xu et al., 2020), we showed that Poisson-based spectral unmixing leads to a more accurate activity estimation (low bias), especially in the low signal-to-noise ratio regime. It is therefore more likely that the dominant effect at the origin of the difference between Genie 2000 and spectral unmixing is the impact of the noise on the activity estimation procedure.

To further highlight this point, we describe in the Appendix 5 an experiment that has been conducted with low level samples. In brief, low level liquid standard sources have been synthesized with 3 radionuclides : ^{210}Pb, ^{137}Cs and ^{54}Mn. The sources only differ in the activity of ^{54}Mn. In contrast to the samples analyzed so far in the article, the spectral signatures are measured, which allows to limit the systematic influence from the spectral signature mismatch. As detailed in Appendix 5 Genie 2000 tends to yield a lower estimation at that low level.

To further assess the sensitivity of spectral unmixing analysis to detect ^{137}Cs at trace level, Table 2 reports the activity estimation of ^{137}Cs for 6 of the 67 measurements. In these measurements, ^{137}Cs is not detected with Genie 2000 but it is with the Poisson based spectral unmixing. To better illustrate these results, the activities are compared to the corresponding decision threshold in Fig. 14. This shows that the detection of ^{137}Cs of these 6 measurements is significant with respect to the decision threshold, whereas they are not with Genie 2000. The result further confirms the sensitivity of the spectral unmixing analysis in real data analysis. The detection rate of low-level activity radionuclide ^{137}Cs increases to 100% from about 80% thanks to the spectral unmixing

analysis, which is a significant improvement in the environmental monitoring work.

5. Conclusion

In this paper, we investigated a new instrument recalibration method for the quantitative analysis of experimental aerosol measurements with HPGe gamma-ray spectrometry with spectral unmixing methods. Along with the determination of characteristic limits with approaches proposed in Xu et al. (2021), this allows to make use of the Poisson-statistics based spectral algorithm as a metrological analysis tool.

To summarize, the quantitative analysis with a given detection system is performed with the following recalibration tasks: i), in the simulation process, the efficiency and the resolution are calibrated so that the simulated spectral signatures can reproduce the actual energy response of the detection system. Furthermore, the measured spectrum need to cope with the spectral contributions due to the specific installations of the detection system (*e.g.*, lead shielding) by adding a spectrum into the spectral signatures' library, ii), an energy calibration refinement step is proposed to correct the energy shift between energy bins of the simulations and the measured spectrum.

The proposed recalibration procedures are evaluated and validated for a detection system with a multi-gamma standard source of known activities. The aerosol measurements performed with this calibrated detection system are subsequently analyzed with the proposed analysis sequence (characteristic limits assessment proposed in Xu et al. (2021) and calibrations). The results are compared to those obtained with Genie 2000 analysis. In conclusion, the Poisson-based spectral unmixing significantly improves the sensitivity of radionuclides' identification in real data analysis, which is particularly required by the rapid detection and rapid characterization of artificial radionuclides (*e.g.*, ^{137}Cs) under emergency conditions.

References

Berlizov, A., 2006. MCNP-CP: A Correlated Particle Radiation Source Extension of a General Purpose Monte Carlo N-Particle Transport Code. volume 945. pp. 183–194. doi:10.1021/bk-2007-0945.ch013.

Briesmeister, J.F. (Ed.), 2000. MCNP: A General Monte Carlo N-Particle Transport Code.

Gilmore, G., 2008. Practical Gamma-ray Spectrometry. 2nd ed., Wiley.

ISO 13528, 2015. Statistical methods for use in proficiency testing by interlaboratory comparison.

Mirion-Canberra, 2016. Genie 2000. URL: https://www.mirion.com/products/genie-2000-gamma-analysis-software.

Wang, C., Zhang, Q., Sun, Y., Liu, J., Zhou, Y., Zhang, M., 2021. A new numerical correction method for gamma spectra based on the system transformation theory of random signals. Applied Radiation and Isotopes 172, 109671. URL: https://www.sciencedirect.com/science/article/pii/S0969804321000816, doi:https://doi.org/10.1016/j.apradiso.2021.109671.

Xu, J., Bobin, J., de Vismes Ott, A., Bobin, C., 2020. Sparse spectral unmixing for activity estimation in γ-ray spectrometry applied to environmental measurements. Applied Radiation and Isotopes 156, 108903.

Xu, J., Bobin, J., de Vismes Ott, A., Bobin, C., Malfrait, P., 2021. Analysis of gamma-ray spectra with spectral unmixing -Part I: Determination of the characteristic limits (decision threshold and statistical uncertainty). URL: https://hal.archives-ouvertes.fr/hal-03345737. working paper or preprint.

Appendix : Comparison between Genie 2000 and spectral unmixing at low level

Analysing mixtures of standard sources

In this article, we suggested that one potential origin of the discrepancy between Genie 2000 and spectral unmixing could be the impact of noise for low level radionuclides. To further test this conjecture, we analyse four synthetic standard sources with known activity concentrations of three radionuclides: ^{210}Pb, ^{137}Cs and ^{54}Mn. To keep the problem somewhat similar to the aerosol filter spectra analysis, ^{210}Pb has an activity level that is customarily observed in aerosol filters (around 100 Bq), while ^{137}Cs and ^{54}Mn have been chosen as substitutes for ^{7}Be and ^{137}Cs with similar energy ranges (662 keV for 477 keV, and 835 keV for 662 keV, respectively) and activity levels. The ^{137}Cs activity level is thus around 1000 Bq. The activity of ^{54}Mn varies in the four sources from 18 mBq to 4.9 Bq. It is important to note that even the lowest activity in our samples is ten times over the activity we usually have in the environment for ^{137}Cs. Unfortunately it was not possible to have sources with certified activities of ^{54}Mn around few mBq, which would correspond to the lowest level of ^{137}Cs in aerosol filters. The spectra of the four mixing sources measured with the studied HPGe are shown in figure 15 with a zoom on the energy range around the characteristic peak of ^{54}Mn. This highlights that this radionuclide is hardly visible for the lowest activity concentration.

Measured spectral signatures

Due to availability and feasibility, we used liquid standard sources in 50 mL vials ($\emptyset$ = 37mm, h = 47mm), instead of the usual 10 mL ($\emptyset$ = 52mm, h = 4.7mm). This implies that the spectral signatures used in the spectral unmixing algorithm cannot be the simulated ones used in the rest of the article. To tackle this problem we have access to mono-radionuclide sources for each of the three radionuclides of the mixing sources. Each of these three sources containing 1000 Bq of one radionuclide was measured for 30 000 s. The measured

spectrum is used as spectral signature in the Φ matrix of the spectral unmixing algorithm. Therefore, calibration errors on the spectral signatures can be considered negligible in this test.

Additionally, this allows to compare the measured spectral signatures can be compared with the spectral signatures calculated by simulation for the 3 radionuclides present in the liquid standard sources. For that purpose the MCNP-CP model was modified by changing the counting geometry from a 10 mL container containing an aerosol filter to a 50 mL containing water, while keeping the HPGe detector unchanged.

As shown in Figure 16 for ^{137}Cs both spectral signatures, measured and calculated, are in very good agreement : the characteristic peak at 662 keV as well as the X-rays of Baryum in the 31.8-36.4 keV range, the Compton continuum shape and the multi-Compton scatterings region (480-662 keV) are perfectly reproduced. The main difference is the Compton edge at 480 keV and the back scattering component at 184 keV. These features have smoother shapes in the measurement due to the Doppler effect: photons do not scatter only on free electrons, as considered in the simulation process. The other difference is the background component in the measured signature over the whole energy range, and the Pb X-rays (72.8 - 87.3 keV) due to the lead shielding which is not simulated.

Estimated activities

We used both Genie 2000 and the spectral unmixing algorithm to analyse the measurement spectra of the four mixing sources. The results are reported in Table 3 with activities (in Bq) and associated uncertainties (in Bq and for $k = 2$) for the 3 radionuclides in the 4 mixing sources : reference values, values estimated by Genie 2000 and values estimated by the spectral unmixing.

as well as in Figures 17 and 18. It is important to note that :

- The estimation made with Genie 2000 and spectral unmixing are similar for high activity radionuclides, as testified by the results obtained for ^{137}Cs

and ^{210}Pb (Fig.17) and the mixtures 3 and 4 (denoted mix 3 and 4 in the figures) that have the highest levels of ^{54}Mn (Fig.18) .

- As shown on Fig. 17 the spectral unmixing estimation is more accurate and more precise than Genie 2000 estimation for ^{210}Pb with estimated value more accurate (ratio close to 1) and uncertainties smaller due to the fact that the information of the full spectrum is used in activity estimation procedure.

- Activity estimation at low level is more challenging; however, the spectral unmixing have better performances than Genie 2000 in this case. Indeed ^{54}Mn is detected even at the lowest level (18 mBq) and the estimation for the second lowest level (49 mBq) is better than the one made with Genie 2000 (see Fig.18).

- The activity of ^{54}Mn is estimated properly by the spectral unmixing for the first mixture (in which the activity of ^{54}Mn is 17.96 ± 0.76 mBq) while it is not detected by Genie 2000, which classifies this radionuclide as having activity under the detection limit (38 mBq).(see Fig.18).

- At low level activity (like the one of ^{54}Mn in mixtures 1 and 2 the information contained in the peaks is not sufficient to estimate the activity of the radionuclides properly. Full spectrum analysis is therefore an appealing solution to this problem in this regime.(see Fig.18).

	source		spectral unmixing		
	reference activity	uncertainty	estimated activity	uncertainty	$\lvert\zeta_{score}\rvert$
^{241}Am	50.4	2.2	50.9	4.3	0.201
^{109}Cd	378	21	376	32	0.114
^{57}Co	18.70	0.64	18.7	1.6	0.004
^{139}Ce	14.89	0.63	14.4	1.2	0.644
^{51}Cr	22.6	1.1	23.0	2.0	0.435
^{113}Sn	37.5	1.7	39.1	3.3	0.877
^{85}Sr	23.51	0.91	25.7	2.2	1.888
^{137}Cs	95.8	3.3	99.5	8.4	0.817
^{88}Y	73.9	2.6	75.9	6.4	0.568
^{60}Co	135.0	4.7	136.5	11.5	0.241
^{210}Pb	353.5	9.3	355	30	0.081

Table 1: Results of the standard source analysis with Poisson based spectral unmixing (Bq). Uncertainty with respect to $k = 2$

Date	09/07/18	11/10/19	21/03/19	18/10/19	25/10/19	17/12/19
Activity	0.136	0.043	0.045	0.058	0.040	0.054
Uncertainty	0.063	0.025	0.016	0.022	0.019	0.021
DT	0.040	0.016	0.009	0.012	0.011	0.011

Table 2: Activity (μBq/m^3) of ^{137}Cs analyzed with spectral unmixing for measurements when ^{137}Cs is not detected with Genie 2000. Uncertainties are assessed with k=2 (2σ), DT = decision threshold.

Mix.	Radionucl.	Reference	Genie 2000	Spectral unmixing
1	Cs-137	1026 ± 39	1022 ± 73	1017 ± 61
	Pb-210	95.9 ± 3.4	101 ± 15	95.8 ± 5.8
	Mn-54	0.01796 ± 0.00076	< 0.038 (DL)	0.02172 ± 0.0071
2	Cs-137	1014 ± 39	1013 ± 72	1008 ± 60
	Pb-210	101.1 ± 3.5	105 ± 15	100.0 ± 6.1
	Mn-54	0.0493 ± 0.0021	0.037 ± 0.018	0.060 ± 0.011
3	Cs-137	993 ± 38	985 ± 70	981 ± 59
	Pb-210	94.4 ± 3.3	102 ± 15	95.3 ± 5.8
	Mn-54	0.485 ± 0.020	0.476 ± 0.069	0.520 ± 0.041
4	Cs-137	1030 ± 39	1024 ± 73	1019 ± 61
	Pb-210	99.8 ± 3.5	105 ± 15	100.5 ± 6.1
	Mn-54	4.92 ± 0.17	5.08 ± 0.51	5.08 ± 0.31

Table 3: Activities and associated uncertainties (k=2) in Bq: certified values of the standard sources (Reference), estimated values by peak based analysis (Genie 2000) and spectral unmixing algorithm. DL refers to the detection limit calculated by Genie 2000 following the ISO 11929 standard ($\alpha = \beta = 0.025$).

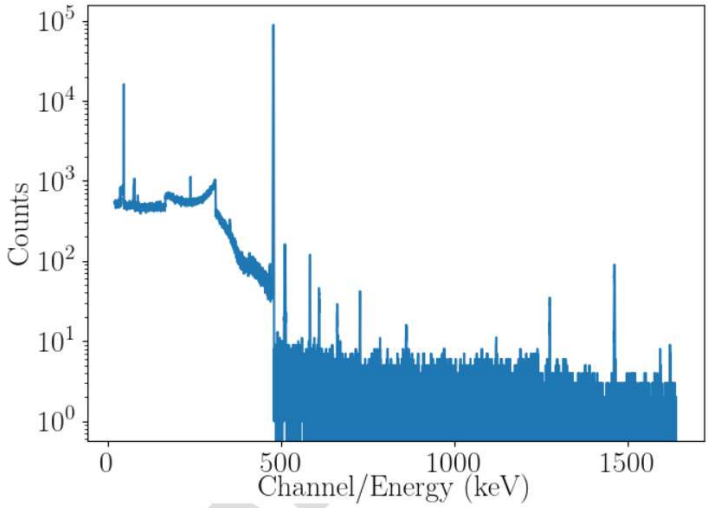

Fig. 1: Example of gamma-ray spectrum of aerosol measurement performed with HPGe detector.

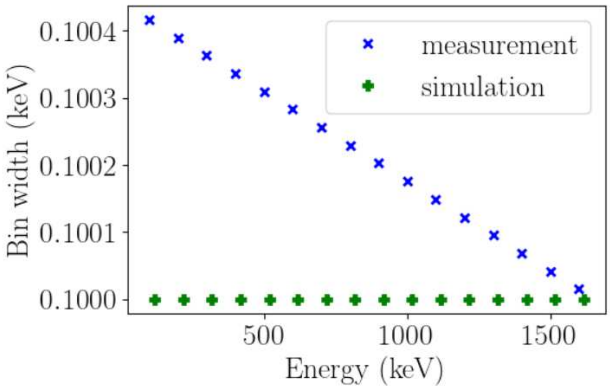

Fig. 2: Energy bin width of simulated spectra and a measured gamma-ray spectrum for several energy bins.

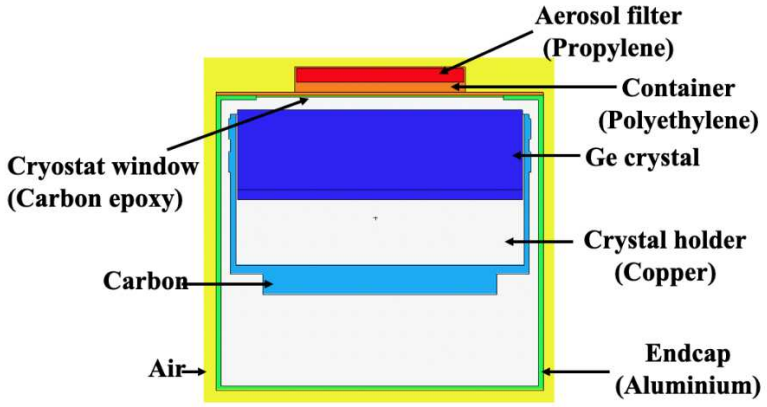

Fig. 3: MCNP-CP simulation model of the detection system.

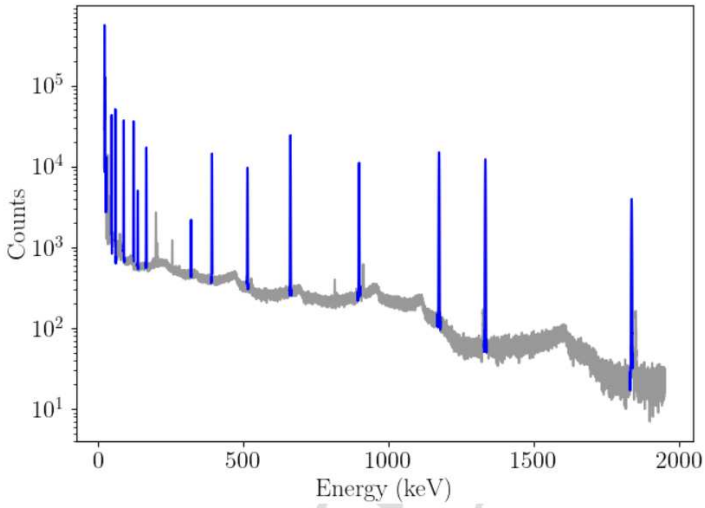

Fig. 4: Measured gamma-ray spectrum of a multi-gamma standard source, which contains ^{51}Cr, ^{57}Co, ^{60}Co, ^{85}Sr, ^{88}Y, ^{109}Cd, ^{113}Sn, ^{137}Cs, ^{139}Ce, ^{210}Pb, ^{241}Am. Peaks for calibrations are shown in blue.

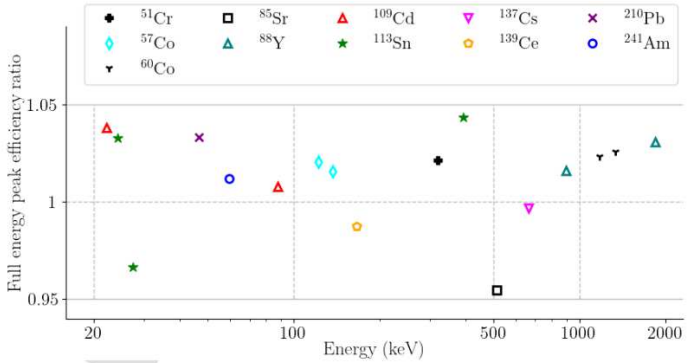

Fig. 5: Ratio between efficiencies determined from simulated spectral signatures and the experimental efficiencies for full energy peaks, different scatters for radionuclides within the source.

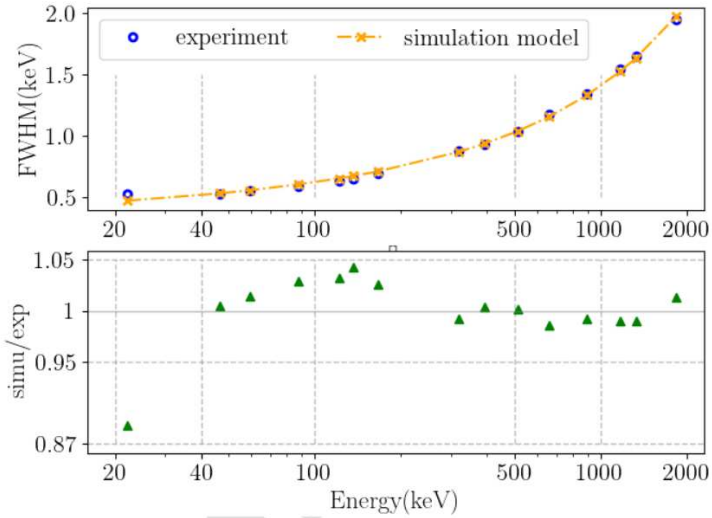

Fig. 6: The resolution fit versus energy. Comparison of $FWHM$ of peaks measured with the standard source and those of fitted with respect to Eq. (6), as well as their ratio.

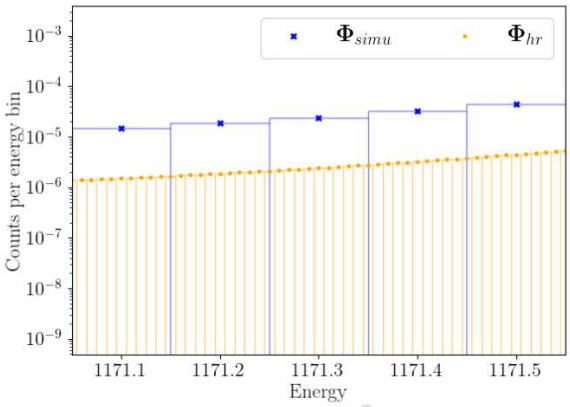

(a) $\mathbf{\Phi}_{hr} = L\mathbf{\Phi}_{simu}$

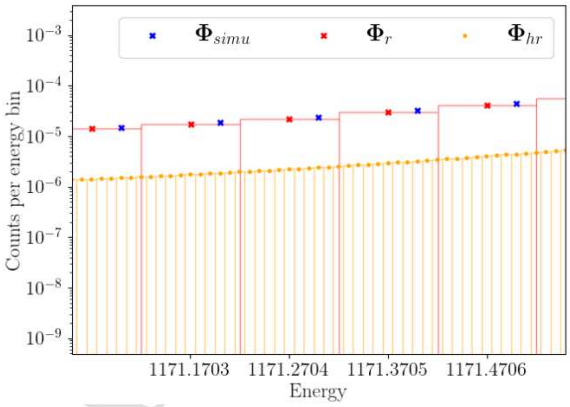

(b) $\mathbf{\Phi}_{r} = H\mathbf{\Phi}_{hr}$

Fig. 7: Illustration of energy bins at which to evaluate the recalibrated values. (a), First interpolation: MCNP-CP simulated spectral signatures (blue) → spectral signatures at high resolution domain(orange), (b) Second interpolation: spectral signatures at high resolution → spectral signatures at energy bins of the measurement(red).

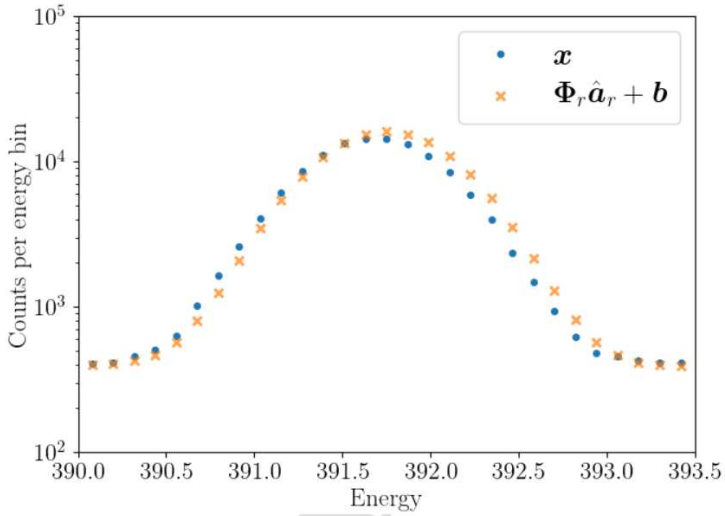

Fig. 8: Energy shift of the spectral unmixing compared to the measured spectrum, where $\boldsymbol{x}$ is the measured spectrum and $\boldsymbol{\Phi}_r\hat{\boldsymbol{a}}_r + \boldsymbol{b}$ is the estimated model with step 2.

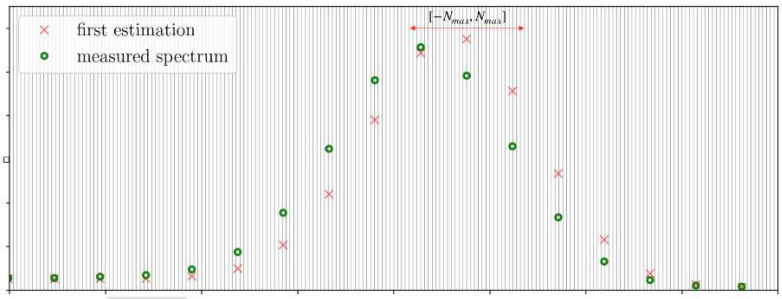

Fig. 9: Illustration of energy shift quantification. Y-axis for the spectrum obtained after the first estimation and the measured spectrum. X-axis for the energy.

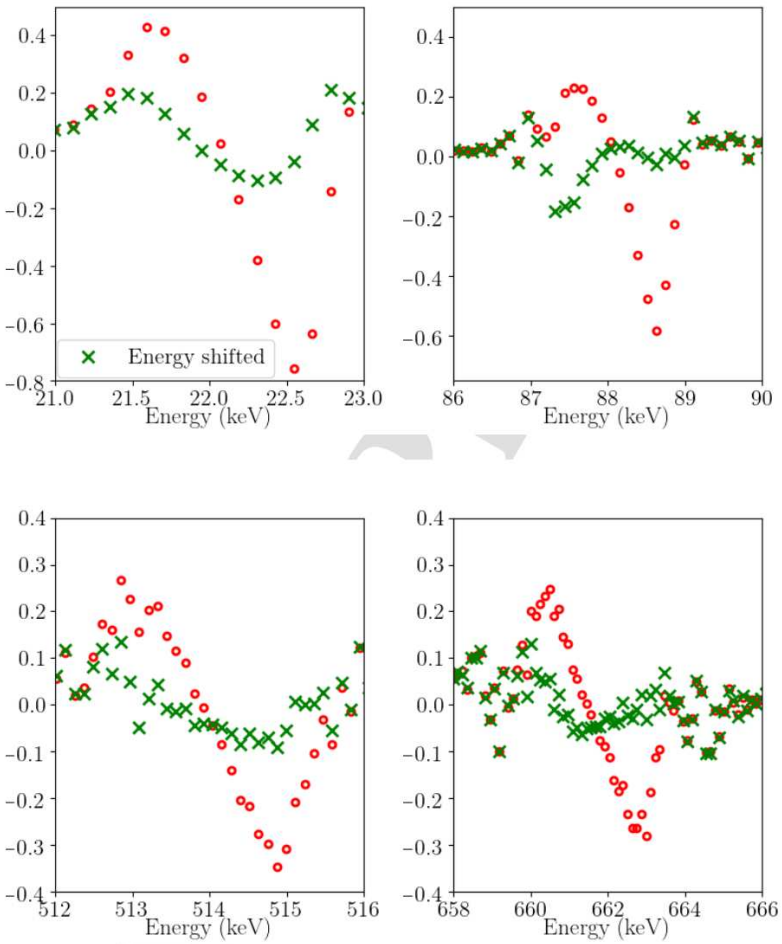

Fig. 10: Evaluation of energy recalibration in zoomed peak regions, with respect to estimation residual normalized by the observed counts: $\frac{x-\Phi a-b}{x}$. The residual before correction and those obtained after correction are display in points (red) and cross (green) respectively in Y-axis as a function of energy.

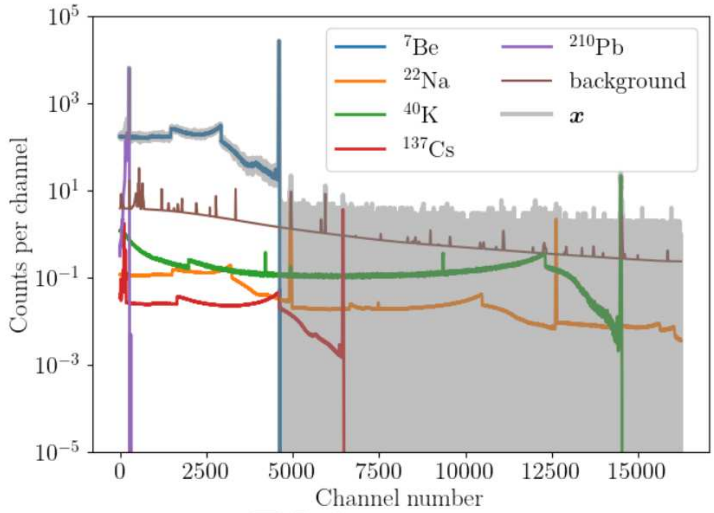

Fig. 11: Simulation of the gamma-ray spectrum of aerosol filter measurement performed with HPGe detector, with realistic radionuclides activities. The measured spectrum $\boldsymbol{x}$ is plotted as a function of the channel number in gray. The spectral contribution of ^{7}Be, ^{22}Na, ^{40}K, ^{137}Cs, ^{210}Pb and the background spectrum are also presented in the figure.

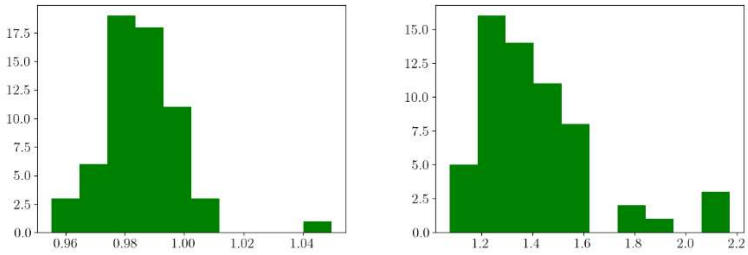

(a) ^{7}Be

(b) ^{22}Na

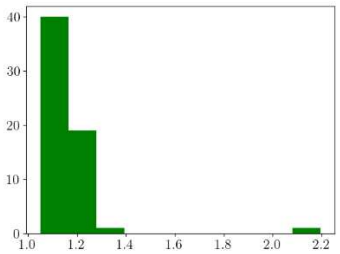

(c) ^{40}K

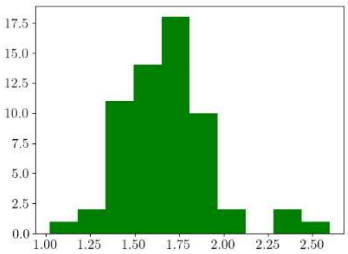

(d) ^{137}Cs

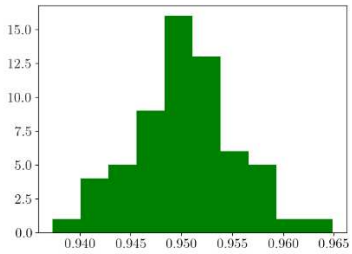

(e) ^{210}Pb

Fig. 12: Histogram of ratio between radioactivity estimation with spectral unmixing and Genie 2000 for 67 aerosols measurements. X-axis for the ratio of results obtained with the two methods and Y-axis for the number of measurements in each range.

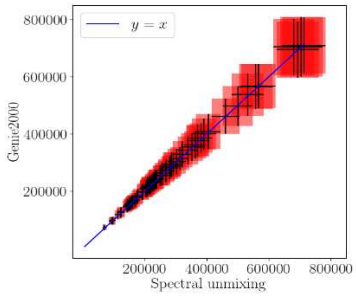

(a) ^{7}Be

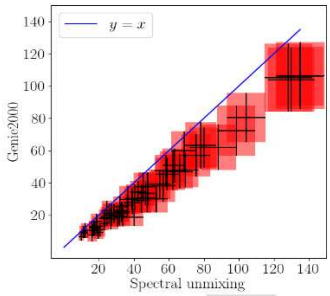

(b) ^{22}Na

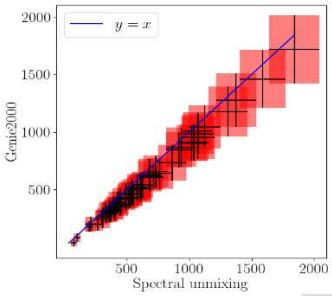

(c) ^{40}K

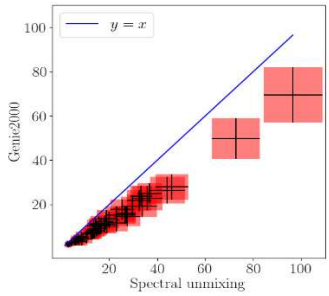

(d) ^{137}Cs

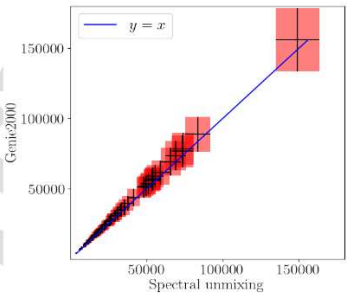

(e) ^{210}Pb

Fig. 13: Activity estimation of aerosol measurements with Poisson-based spectral unmixing and Genie 2000. Error bars for activity (mBq) ± uncertainty (k=2) for each measurement.

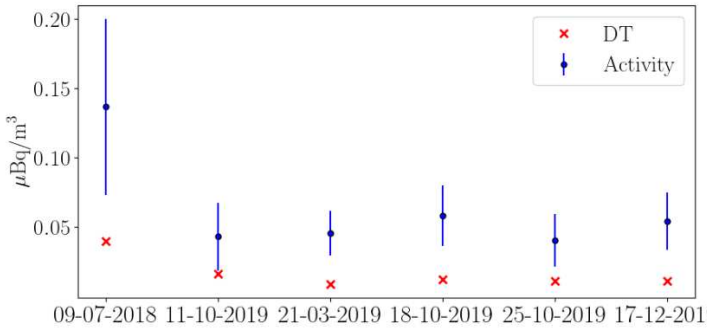

Fig. 14: Results obtained with Poisson based spectral unmixing. Activity $\pm$ uncertainty of ^{137}Cs (blue), the decision threshold (red).

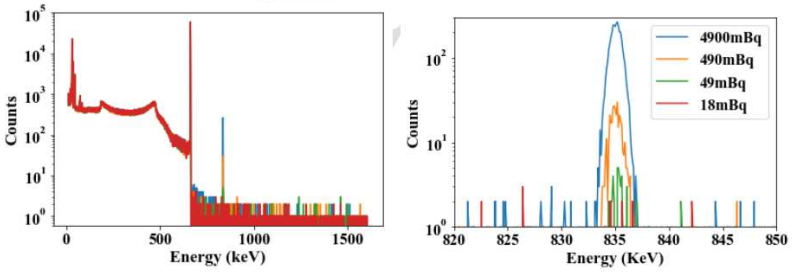

Fig. 15: Spectra of the four standard sources measurements for 30 000 s with the studied HPGe detectors (left) and zoom in on the region of the ^{54}Mn characteristic peak (right). The four liquid sources are contained in 50 mL vials and have the same activity of ^{137}Cs and ^{210}Pb and (1000 and 100 Bq, respectively). The activity level of ^{54}Mn is the only one that changes in the sources from 0.018 Bq to 4.9 Bq.

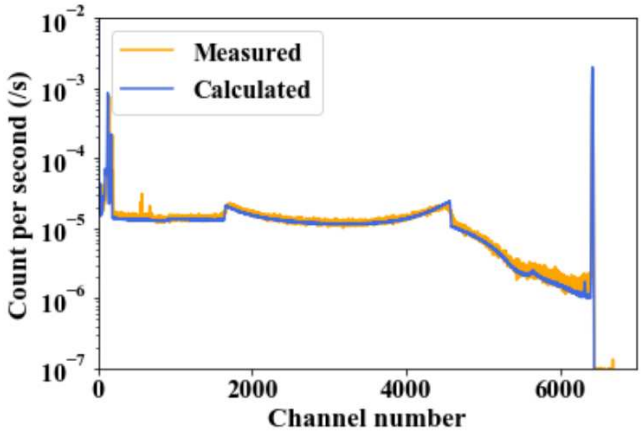

Fig. 16: Comparison between measured and calculated spectral signatures for ^{137}Cs contained in a 50 mL vial and measured on the studied HPGe detector. The measured signature were obtained by measuring for 30 000 s a liquid standard source containing 1000 Bq of ^{137}Cs. The calculated signature was obtained using the MCNP-CP code simulating the disintegration of ^{137}Cs.

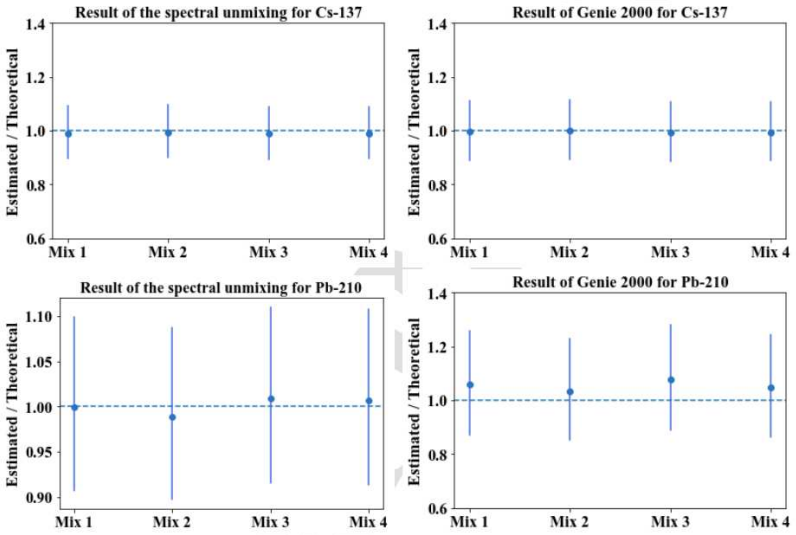

Fig. 17: Ratios between the estimated activities and the reference valuers with uncertainties (k=2). Results are presented for both analysis methods (spectral unmixing on left and Genie 2000 on right) for both radionuclides present at highest levels : ^{137}Cs (top) and and ^{210}Pb (bottom) at 1000 Bq and 100 Bq respectively.

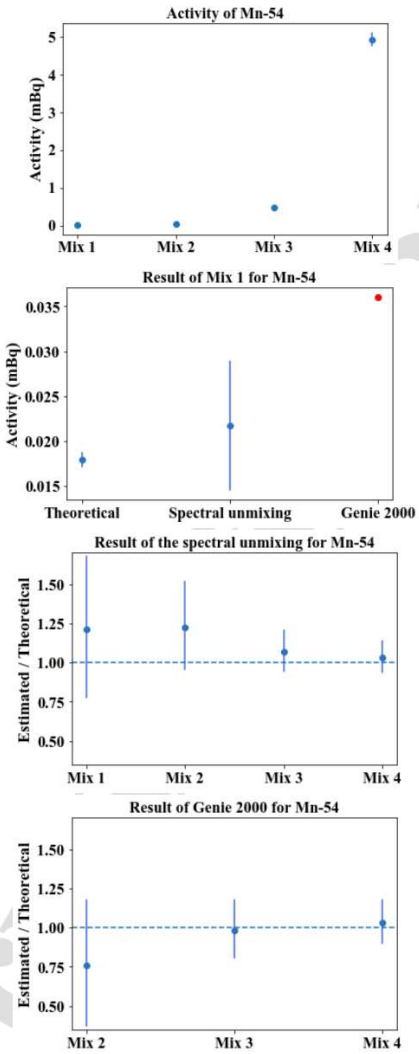

Fig. 18: Results of spectral unmixing (bottom-left) and Genie 2000 (bottom-right) on the different sources for ^{54}Mn with varying activities (top-left). Results for the first source with very low activity (18mBq) are compared on the top-right figure with the reference value, the value estimated by spectral unmixing and the detection limit (38 mBq) calculated by Genie 2000 following the ISO 11929 standard ($\alpha = \beta = 0.025$), in red.

- Instrument recalibration methods for gamma-ray spectrometry with spectral unmixing
- Efficiency and resolution recalibrations in the simulation process
- Correction of the energy shift between both simulated and measured spectra
- Validation of the recalibration procedure with a standard source measurement
- Application to real data of aerosol filters measurements

Declaration of interests

☒ The authors declare that they have no known competing financial interests or personal relationships that could have appeared to influence the work reported in this paper.

☐The authors declare the following financial interests/personal relationships which may be considered as potential competing interests: